

# THE BEAM OPTICS OF THE FFAG CELL OF THE CBETA ERL ACCELERATOR\*

N. Tsoupas<sup>†</sup>, J. S. Berg, S. Brooks, George Mahler, F. Méot, V. Ptitsyn, D. Trbojevic  
 Brookhaven National Laboratory, Upton NY, USA  
 S. Tygier, University of Manchester, Manchester, UK  
 J. Crittenden, Cornell University, Ithaca, NY, USA

## Abstract

The CBETA project [1] is a prototype electron accelerator for the proposed eRHIC project [2]. The electron accelerator is based on the Energy Recovery Linac (ERL) and the Fixed Field Alternating Gradient (FFAG) principles. The FFAG arcs and the straight section of the accelerator are comprised of cells with one focusing quadrupole and one combined function defocusing quadrupole. Both cell magnets are Halbach type permanent magnets [3]. We will present the beam optics of the FFAG cell which is based on 3D field maps which are derived with the use of the OPERA computer code [4]. We will also present the electromagnetic design of the correctors of the FFAG's cell magnets.

## INTRODUCTION

The approved and funded CBETA project [1], which is currently under construction at Cornell University is an electron accelerator which combines two remarkable concepts, the Energy Recovery Linac (ERL) and the Fixed Field Alternating Gradient (FFAG) concept. The accelerator consists of a 1.3 GHz 80 MeV Linear accelerator and one recirculating beam line. Fig. 1 is a layout of the electron accelerator with the various sections labelled, Injection section (IN) Linear accelerator section (LA), splitter-merger (SX, RX), recirculating section (FA, TA, ZA, ZB, TB, FB) and the beam dump section (BS). The present design of the CBETA calls for 150 MeV maximum beam energy of the electron bunches. This energy will be achieved by injecting into the ERL electron bunches of 6 MeV of energy and accelerating each bunch by 36 MeV each time the electron bunch passes through the ERL as it is recirculated in the single FFAG arc. After the electron bunches reach their top energy of 150 MeV, the bunches are recirculated back into the ERL, each time delivering 36 MeV of energy to the LINAC until they reach the 6 MeV energy to be dumped in the BS line shown in Fig. 1. Thus with the use of the ERL concept we can accelerate electrons to a high energy with a minimal power consumed in the LINAC since almost all of the LINAC energy required to accelerate the electron bunches is obtained from the decelerated electron bunches. The FFAG concept employed in the CBETA accelerator allows the recirculating electron bunches in the range of 42 to the 150 MeV to be confined in a

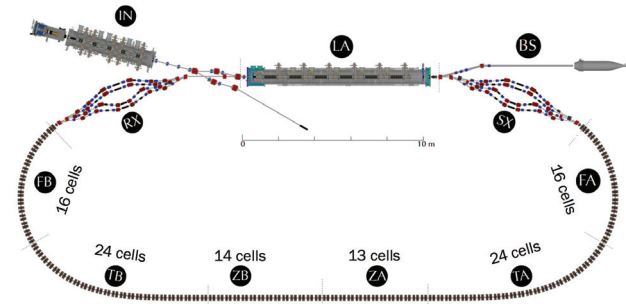


Figure 1: Layout of the CBETA accelerator. The section labeled (LA) is the ERL, The sections labeled (FA), (TA), (ZA), (ZB), (TB), and (FB) are the FFAG sections which accommodate four recirculating electron bunches which have an energy range from 42 MeV to 150 MeV.

smaller than 4.66 cm transverse good field region generated by the permanent magnets of the FFAG doublet cell.

## THE FFAG CELL OF THE CBETA ACCELERATOR

The FFAG arcs (FA, FB in Fig. 1), transition (TA, TB), and FFAG straight sections (ZA, ZB) of the CBETA accelerator consists of doublet cells, each cell comprised of one focusing pure quadrupole and one defocusing quadrupole with an additional dipole component. In Fig. 2 the trajectories of the electron bunches are shown for the energy range of 42 to 150 MeV. The maximum transverse displacement between these bunches is less than 4.66 cm. This is the remarkable property of the FFAG which places electron bunches with large energy range into a relatively small transverse space of the doublet cell. In Fig. 2 the labeled rectangle QF is the pure focusing quadrupole and rectangle labeled BD is the defocusing quadrupole with the dipole component. Prerequisite to the study of the FFAG cell's beam optics is the study of the magnetic fields generated by the elements of the FFAG cells. In the next subsection we will present results from the 2D and 3D electromagnetic calculations of the the pure focusing quadrupole Halbach type magnet and the defocusing quadrupole magnet with a dipole component.

### *The 2D and 3D Electromagnetic study of the QF and BD elements of the FFAG cell*

To generate the final beam optics of the cell we follow an iterative process, starting with 'hard edge' magnets which must provide the required multipoles. Subsequently a 2D

\* This manuscript has been authored by employees of Brookhaven Science Associates, LLC under Contract No. DE-SC0012704 with the U.S. Department of Energy. This work was performed with the support of NYSERDA (New York State Energy Research and Development Agency).

<sup>†</sup> tsoupas@bnl.gov

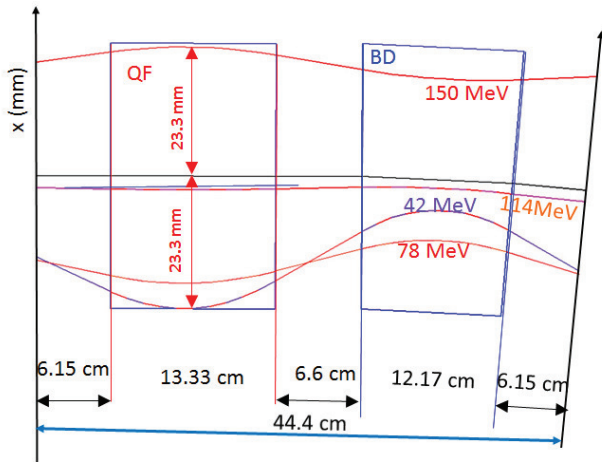


Figure 2: A schematic diagram of the FFAG doublet cell showing the trajectories of the electron bunches ranging in energy from 42 to 150 MeV in constant magnetic field. The label QF designates the pure focusing quadrupole and the label BD the defocusing quadrupole with the dipole component.

model of the magnet is generated to provide these multipoles followed by a 3D model of the magnet that provides the required 3D field map for the beam optics calculations. Few iterations are required to finalize the 3D design of the magnet which will provide the optimum beam optics. In the next two subsections we provide results from the 2D and 3D electromagnetic calculations.

**The 2D design** From the beam optics calculations which are based on ‘hard edge’ magnets we obtain the required multipoles of the magnets. The 2D electromagnetic calculations determine the cross section of the cell magnets which provide these multipoles. Fig. 3 is the cross section of the focusing quadrupole (QF) on the left, and the defocusing quadrupole (BD) on the right with a dipole component. The black lines on the figures are the equipotential vector lines. The QF is pure quadrupole Halbach type magnet which is made of 16 wedges and its quadrupole component is given by [5]

$$2B_{rm} \cos^2\left(\frac{\pi}{M}\right) \frac{\sin\left(\frac{2\pi}{M}\right)}{\left(\frac{2\pi}{M}\right)} \left(\frac{1}{r_i} - \frac{1}{r_o}\right) \quad (1)$$

In Eq. (1)  $B_{rm}$  is the remnant magnetization,  $r_i$  and  $r_o$  the inner and outer radii of the annulus made by the wedges, and  $M$  is the number of magnetized wedges. The magnetization direction  $\alpha$  of each of the wedges is given by  $\alpha = 3\theta + \frac{\pi}{2}$ , where  $\theta$  is the azimuthal angle of each wedge.

The BD magnet which can provide the quadrupole and the dipole field can be made as a superposition of two layers of Halbach magnets each layer made of 16 wedges. In this paper we present an alternative 2D design of the BD magnet [6] which consists of a single layer of 16 wedges of varying

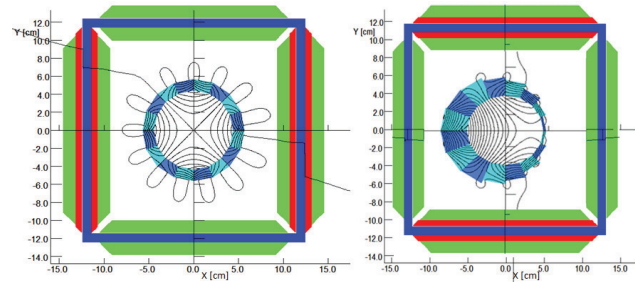


Figure 3: The cross sections of the (QF) a pure focusing Halbach magnet (left), and the (BD) a defocusing quadrupole magnet with a dipole component (right). Both QF and BD Halbach magnets have window frame electromagnets as correctors.

transverse size. The 2D computer code which optimizes the design is available upon request [6].

The window frame magnets around the (QF) and (BD) magnets, have coils which provide a normal dipole (red areas) and a normal quadrupole (green areas). By rotating the window frame magnet by  $90^\circ$  we can generate a skew dipole.

**The 3D design** The 3D electromagnetic design of the magnets is an essential part of the beam optics calculations because it provides an accurate description of the field generated by the magnets of the cell taking into account the fringe fields, and the contribution to the magnetic field from the magnets of the neighboring cells. Table 1 contains the geometry of the QF and BD magnets which generate the required fields to satisfy the beam optics requirements. The

Table 1: Cell Magnets Specifications: The inner and outer radii the length and the dipole and quadrupole multipole strengths generated by the QF and BD magnets of the cell.

Mag	Ri[mm]	Ro[mm]	L[mm]	D[T]	Q[T/m]
QF	44.05	56.51	121.7	0.0	11.43
BD	44.05	varies	133.3	-0.317	10.87

beam optics calculations provide the relative positions of the QF and BD magnets within the FFAG cell. This information is used in the OPERA code to generate the 3D model of the cell. Fig. 4 shows an isometric view of a model with three consecutive cells. The field map of the middle cell is used in the beam optics calculations.

### Arc Cell Design

The magnets described here were used to produce a final arc cell design. The final geometry is related to our beam pipe configuration and the desired path length. The beam pipe consists of straight segments which meet 42 mm long BPM blocks where a 5 degree bend occurs (2.5 deg. on either side of the block). Other parameters are chosen based on space constraints and to leave sufficient space for instrumentation. Some parameters were retained from earlier design

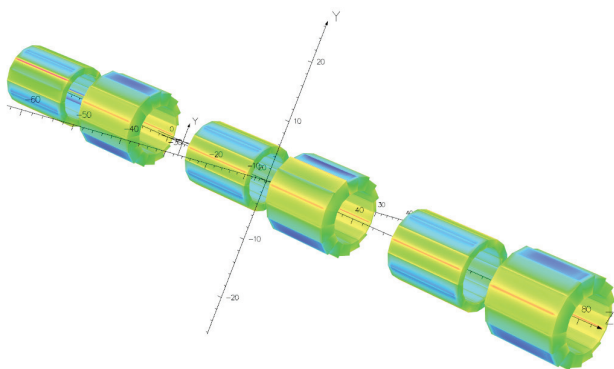


Figure 4: Isometric view of model with three consecutive FFAG cells. The field map of the middle cell is used in the beam optics calculations.

Table 2: Parameters for the arc cell

BPM block length (mm)	42
Pipe length (mm)	402
Magnet offset from BPM block (mm)	12
Focusing quadrupole length (mm)	133
Defocusing magnet length (mm)	122
Single cell horizontal tune, 42 MeV	0.368
Single cell vertical tune, 150 MeV	0.042
Integrated focusing magnet strength (T)	-1.528
Integrated defocusing magnet strength (T)	+1.351
Integrated field on axis, defocusing (T m)	-0.03736

versions. The overall length was adjusted to achieve a desired machine circumference considering the entire machine as a whole. Our tracking studies indicated concerns with the  $\nu_x + 2\nu_y = 1$  resonance [7], and we wish to avoid other third-order resonances, as well as vertical instability at high energy. Our final parameters chosen are shown in Table 2. Once the longitudinal lengths are fixed, there are three free parameters: two magnet gradients, and the dipole field in the defocusing magnet. The parameters are chosen so that the maximum horizontal closed orbit excursion at 150 MeV and the minimum horizontal closed orbit excursion at 42 MeV, relative to the line defining the coordinate system, are of equal magnitude and opposite sign.

The remaining two degrees of freedom are used to set the tunes at the working energies. High horizontal and low vertical tunes generally reduce orbit excursions and magnet gradients. However, one must avoid the horizontal half-integer resonance at low energy and becoming linearly unstable at high energy in the vertical plane. We have chosen our working point in the tune plane by considering how much the gradients would need to change to reach problematic resonance lines. We quantify this change by

$$\sqrt{(\Delta G_F/G_F)^2 + (\Delta G_D/G_D)^2} \quad (2)$$

where  $G_F$  ( $G_D$ ) refers to the gradient of the (de)focusing magnet. We find the minimum value for this quantity for values meeting the resonance condition in question, and define

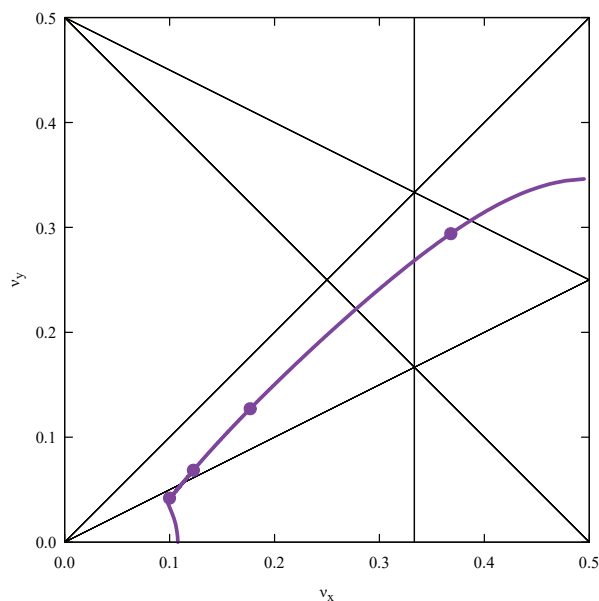


Figure 5: Tune per cell for the arc cell, treated as periodic. Design energies are shown with dots.

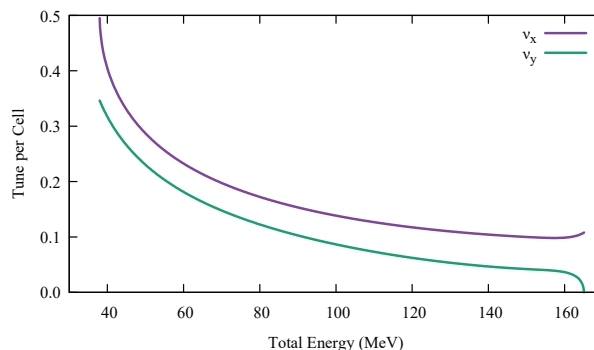


Figure 6: Tune per cell for the arc cell, treated as periodic, as a function of energy.

that to be the parametric distance. The working point is chosen so that the parametric distance from the 150 MeV point to the  $\nu_y = 0$  line is approximately equal to the parametric distance from the 42 MeV point to the  $\nu_x + 2\nu_y = 1$  line, and the parametric distances from the 150 MeV and 114 MeV points to the  $\nu_x - 2\nu_y = 0$  line are about the same. The resulting working point is reasonably well-defined by the 42 MeV horizontal and 150 MeV vertical tunes, which are given in Table 2. The parametric distance to the  $\nu_x + 2\nu_y = 1$  line is 3.0%, to the  $\nu_y = 0$  line is 3.8%, and to the  $\nu_x - 2\nu_y = 0$  line is 1.3% (114 MeV) and 1.2% (150 MeV).

Beginning with the field maps described above, we scale and shift them to achieve the desired orbit centering and tune working point. Magnet designs are then modified to have the resulting integrated gradient and central field, field maps are computed from those designs, and the results are checked (and were found to be in good agreement). Figures 5 and 6 show the tune per cell for the arc cell.

**REFERENCES**

- [1] <http://arxiv.org/abs/1504.00588>
- [2] <http://arxiv.org/abs/1409.1633>
- [3] K. Halbach, "Design of permanent multipole magnets with oriented rare earth cobalt material", Nucl. Instrum. Meth. 169 (1980) pp. 1-10.
- [4] <http://www.scientificcomputing.com/company-profiles/vector-fields-inc>
- [5] S.M. Lund and K. Halbach "Iron free permanent magnet systems for charged particle beam optics" UCRL-JC-121454 (1995)
- [6] S. Brooks private communication, sbrooks@bnl.gov
- [7] F. Méot, S. Brooks, D. Trbojevic, N. Tsoupas, and S. Tygier, "Numerical Beam Dynamics Studies Regarding CBETA Cornell-BNL ERL," presented at the 8th International Particle Accelerator Conference (IPAC'17), Copenhagen, Denmark, May 2017, paper MOPIK123, this conference.